J Electroceram (2006) 17:277–281
DOI 10.1007/s10832-006-7729-7

Structural and electrical properties of low resistance Pt/Pd/Au contact on p-GaN

Young Soo Yoon · Han-Ki Kim

Received: 2 August 2005 / Revised: 22 November 2005 / Accepted: 10 February 2006
© Springer Science + Business Media, LLC 2006

Abstract We have investigated electrical and structural properties of Pt/Pd/Au ohmic contact on *p*-type GaN:Mg (2.5×10^{17} cm^{-3}) using Auger electron spectroscopy (AES) and glancing angle x-ray diffraction (GXRD) analysis. It was shown that the specific contact resistivity improved with increasing annealing temperature. The annealing of the contact at 600°C for 2 min in flowing N_2 atmosphere resulted in a specific contact resistivity of $3.1 \times 10^{-5}\ \Omega\,\mathrm{cm}^2$. Both GXRD and AES depth profile results show that Ga_3Pt_5, Ga_2Pd_5, and Au_7Ga_2 phases are formed at the interface region between metal and GaN when annealed at temperatures 600°C. Possible explanation is suggested to describe the annealing dependence of the specific contact resistivity of the Pt/Pd/Au contacts.

1 Introduction

The fabrication of high quality ohmic contacts on both n- and p-type GaN layers is essential for high quality light emitting diodes (LEDs), laser diodes (LDs), and ultra violet detectors [1–4]. In particular, there has been much efforts for developing low resistance, thermally stable and reliable ohmic contacts to p-GaN [5–8]. The most common approach for ohmic contact on p-GaN is believed to proceed by the formation of a heavily doped interface layer upon annealing of an Ni-, Pd-, and Pt-based metal system that enhances field emission transport through the contacts [7, 9–11]. Other approaches aim at lowering the Schottky barrier height (SBH) by chemical passivation and removal of oxide layer on p-GaN [12–14]. More recently, promising approaches using Ni-based alloys such as Ni-La, Ni-Zn, Ni-Mg, and Ni-Cu produced very low specific contact resistivity in $10^{-5}\sim10^{-6}\ \Omega\,\mathrm{cm}^2$ range, depending on metal schemes [15–18]. From those approaches, Ni/Au is although being used as p-contact electrode for conventional InGaN/GaN LEDs, various Pt- and Pd- based ohmic contact such as Pt/Ni/Au, Pt/Ru, Pt, Pt/Au, Ti/Pt/Au, Pd/Au, Pd/Ni, Pd/Pt/Au, Pt/Pd/Au, and Pd/Ag/Au/Ti/Au also have been investigated significantly due to the fact that those metals have large work functions and easily react with gallium during an annealing process [7, 13, 19–29]. The specific contact resistivities of both the Pt- and Pd-based ohmic contacts are typically in the range of low $10^{-3}\sim10^{-5}\ \Omega\,\mathrm{cm}^2$. However, detailed examinations about the electrical and structural properties of a Pt/Pd/Au scheme containing both Pt and Pd layers on p-GaN have not been performed so far. To understand the exact ohmic contact mechanism of the Pt/Pd/Au scheme on the p-GaN, it is important to understand detailed interfacial reaction between Pt/Pd/Au and *p*-GaN with increasing annealing temperature.

In this work, we have investigated the electrical and structural properties of the Pt/Pd/Au contact on p-GaN as a function of the annealing temperature. Both GXRD and AES depth profile results showed that the formation of the Ga_3Pt_5, Ga_2Pd_5, and Ga_2Au_7 phases at the interfacial region played an important role in reducing specific contact resistivity. Based on AES and GXRD analysis, we suggested a possible mechanism to describe temperature dependence of the Pt/Pd/Au contact on *p*-GaN.

Y. S. Yoon
Department of Advanced Technology Fusion (DATF), Konkuk University, 1 Hwayang-dong, Gwangjin-gu, Seoul 143-701, Korea
e-mail: ysyoon@konkuk.ac.kr

H.-K. Kim (✉)
School of Advanced Materials and Systems Engineering, Kumoh National Institute of Technology (KIT), 1 Yangho-dong, Gumi, Gyeongbuk, 730-701, Korea
e-mail: hkkim@kumoh.ac.kr

2 Experimental

Some 1 μm-thick p-GaN:Mg layers was grown on a 1 μm-thick undoped GaN buffer layer by metalorganic chemical vapor deposition. The as-grown p-GaN samples were then rapid-thermal-annealed at 850 °C for 3 min in nitrogen ambient to activate the Mg dopants. A carrier concentration and a mobility were measured to be 2.5×10^{17} cm^{-3} and 9.85 cm^2/Vs, respectively, by Hall measurements at room temperature. The p-GaN layer was ultrasonically degreased with acetone, methanol, and methanol for 5 min in each step, and then rinsed with deionized water followed by N_2 blowing. The p-GaN layers were then boiled in a buffered hydrofluoric (BHF) solution for 10 min to remove surface oxide layers [29]. For the measurement of contact resistivity, an active region was defined by inductively-coupled-plasma reactive ion etching (ICP-RIE) using a mixture of BCl_3/Cl_2/Ar gases. Rectangular TLM patterns were transferred on electrically isolated mesa pads by a standard photolithographic technique. The size of the contact pads was 70 × 100 μm and the spacings (d) between the pads were 2, 3, 4, 5, 6, 8, and 10 μm. Prior to metal film deposition, the surface of p-GaN was dipped in BHF solution for 1 min and blown dry in N_2. Thin Pt (7 nm)/Pd (7 nm)/Au (15 nm) films were deposited by electron beam evaporation. After metal deposition, the samples were rapid-thermal-annealed at temperatures in the range of 400–600°C for 2 min in nitrogen ambient (JIPELEC). Current-Voltage (I-V) characteristics were measured using a four-probe arrangement at room temperature. AES depth profile examination was performed using a PHI 670 Auger microscope with electron beam of 5 keV and 0.0236 μA. The interfacial reaction products were further characterized by GXRD using Cu Kα radiation, which was carried with a Rigaku diffractometer (D/MAX-RC).

3 Results and discussion

The typical I-V characteristics of the Pt/Pd/Au ohmic contacts on p-GaN as a function of the annealing temperature, measured between the pads with a spacing of 3 μm are shown in Fig. 1. It was shown that the as-deposited sample exhibited a non-linear *I-V* characteristic due to the large work function of the p-GaN (>7.5 eV) [27, 28]. However, the linearity of the I–V curves becomes improved with increasing annealing temperature. It can be seen that the contact became ohmic at annealing temperature above 500°C. The contact resistance (R_c) and the sheet resistance (R_s) were determined from the intercept of the y-axis and the slope of total resistance R_T versus the pad spacing. The specific contact resistivity was calculated by $\rho_c = R_c^2 / R_s$. The as-deposited sample reveals a rectifying behavior. However, 600 °C annealed sample yield

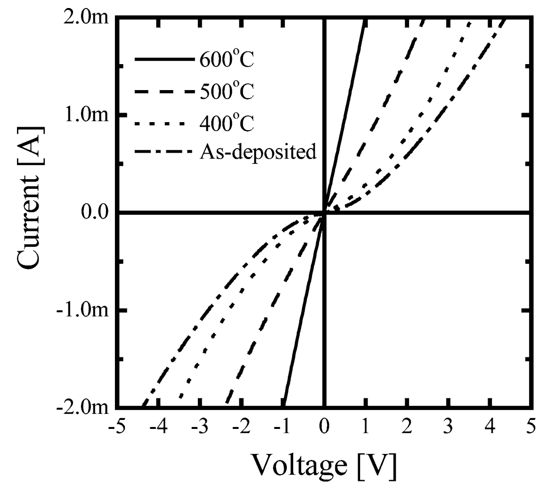

Fig. 1 The current-voltage characteristics of the Pt/Pd/Au contacts on p-GaN as a function of the annealing temperature

a specific contact resistivity of $3.1 \times 10^{-5}\ \Omega\,\mathrm{cm}^2$. It was noted that the sample annealed at 600 °C shows the best I-V characteristic. In our previous work, Pt/Pd/Au contacts on p-AlGaN was found to produce the best I-V characteristics with specific contact resistivity of a $3.1 \times 10^{-4}\ \Omega\,\mathrm{cm}^2$ after 600°C annealing [27]. It is noteworthy that the Pt/Pd/Au ohmic contact on p-GaN results in higher contact resistivity by one order of magnitude, compared to the Pt/Pd/Au ohmic contact on p-AlGaN. It is thought that the different behavior of the Ga outdiffusion from p-GaN and p-AlGaN lead to a difference in a specific contact resistivity. Murai et al investigating the effect of Pd or Pt addition to Ti/Au ohmic contact of n-AlGaN reported that the addition of Pd of Pt layer resulted in a formation of Pd-Ga or Pt-Ga compound after annealing at 600°C [28]. This indicates that Ga outdiffusion in AlGaN occurs much higher annealing temperature than Ga outdiffusion in conventional GaN contact (∼400°C) due to difference of binding energy and structure of Ga atom with Al and N atoms.

Figure 2(a) shows the AES depth profiles of the as-deposited Pt/Pd/Au contacts on p-GaN. It was shown that individual layers of Pt, Pd, and Au are well defined, indicating the absence of significant interfacial reactions between the metal and GaN. However, it is worth noting that a small amount of Ga atoms outdiffused from the GaN layer. GXRD examination was also made of the as-deposited sample to characterize interfacial reaction product in Fig. 2(b). The GXRD plot reveals the diffraction peaks of Pt, Pd, and Au, as expected from AES results in Fig. 2(a). Due to the similar lattice constants and structure of the Pt and Pd metal layers and resolution limits, there is overlapping in the diffractions peaks of the Pt and Pd.

Figure 3(a) shows the AES depth profile of the sample annealed at 400°C. The profile illustrate that some amount of

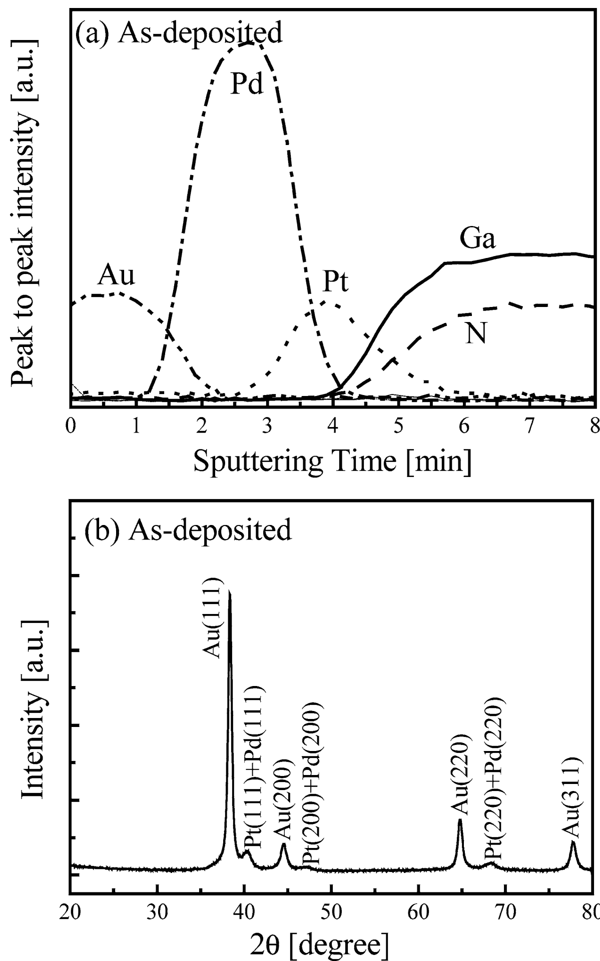

Fig. 2 (a) The AES depth profile of the as-deposited Pt/Pd/Au contact on the *p*-GaN layer. (b) The GXRD results of the as-deposited contact

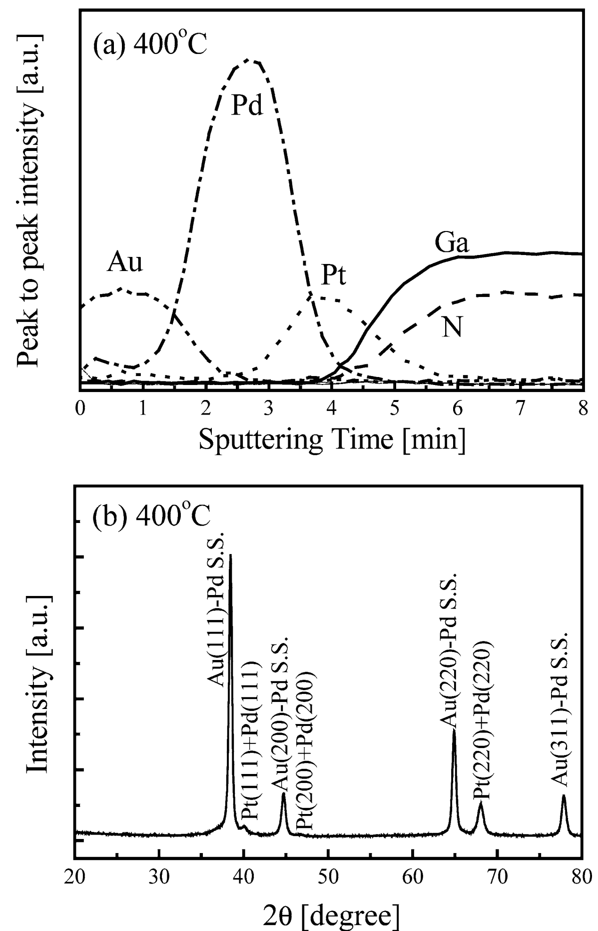

Fig. 3 (a) The AES depth profile of the sample annealed at 400°C. (b) The GXRD results of the sample annealed at 400°C, showing an increased peak intensity compared to as-deposited sample

Pd outdiffused to the surface the sample through Au layer and also diffused into Pt layer. There is no obvious evidence for the outdiffusion of N atoms into the metal layer. Figure 3(b) shows the GXRD plot of the sample annealed at 400°C. Compared to the GXRD plot of the as-deposited sample, it can be seen that there is no significant change. However, the intensity of the Au based-Pd solid solution (Au-Pd S.S.) ($2\theta = 38.35°, 44.71°, 64.88°, 77.86°$) and Pt (200) + Pd (200) ($2\theta = 68.01°$) peaks was drastically increased due to the crystallization of Au layer and interface reaction of Pt and Pd layer as expected from AES depth profile.

Figure 4(a) shows AES depth profile of the sample annealed at 500°C. Compared to 400°C sample, more Pd atoms outdiffused to the sample surface and participated in the formation of an Au based-Pd solid solution. In addition, it is shown that Pd diffused into the interface region between metal and GaN and reacted with Pt and Ga atoms and lead to formation of Pt-based Pd solid solution and Pd-Ga phases. Figure 4(b) exhibits the GXRD plot of the sample annealed at 500°C. As expected from AES depth profile, in addition to the phases observed in 400°C-annealed sample, there are new diffraction peaks, which were identified to be Ga_3Pt_5 (001)(22.44°), Ga_3Pt_5 (220)(33.01°), Ga_3Pt_5 (221)(40.13°), Ga_3Pt_5 (440)(68.08°), Ga_3Pt_5 (600)(70.77°), Ga_2Pd_5 (330)(52.08°), Ga_2Pd_5 (220)(57.24°), and Ga_2Pd_5 (123)(71.99°). The occurrence of these additional phases seems to be consistent with the extensive interfacial reactions between thin Pt/Pd and GaN atoms. In addition, the intensity of Au-based and Pd-based solid solution peaks was significantly increased by further crystallization during annealing process.

Figure 5(a) shows the AES depth profile of the sample annealed at 600°C, which is best annealing condition to obtain lowest specific contact resistivity using a Pt/Pd/Au scheme. For the sample annealed at 600°C, a significant amount of Pd atoms indiffused toward the interfacial region and outdiffused toward the sample surface through the top Au layer. In addition, some amounts of the Pt atoms also react with Ga atoms, which are outdiffused from the *p*-GaN. This indicates

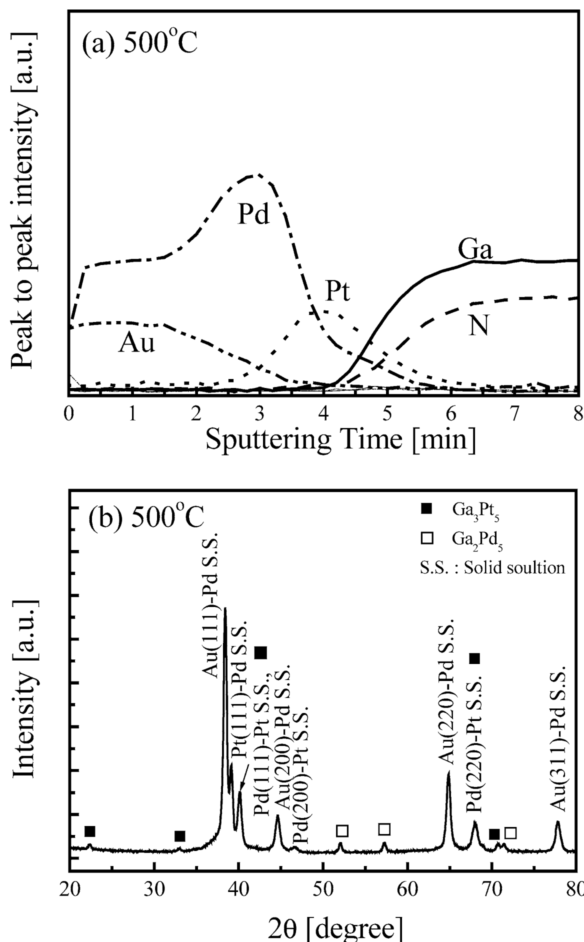

Fig. 4 (a) The AES depth profile of the sample annealed at 500°C. (b) The GXRD results of the sample annealed at 500°C, showing the formation of new phases such as Ga_3Pt_5 and Ga_2Pd_5

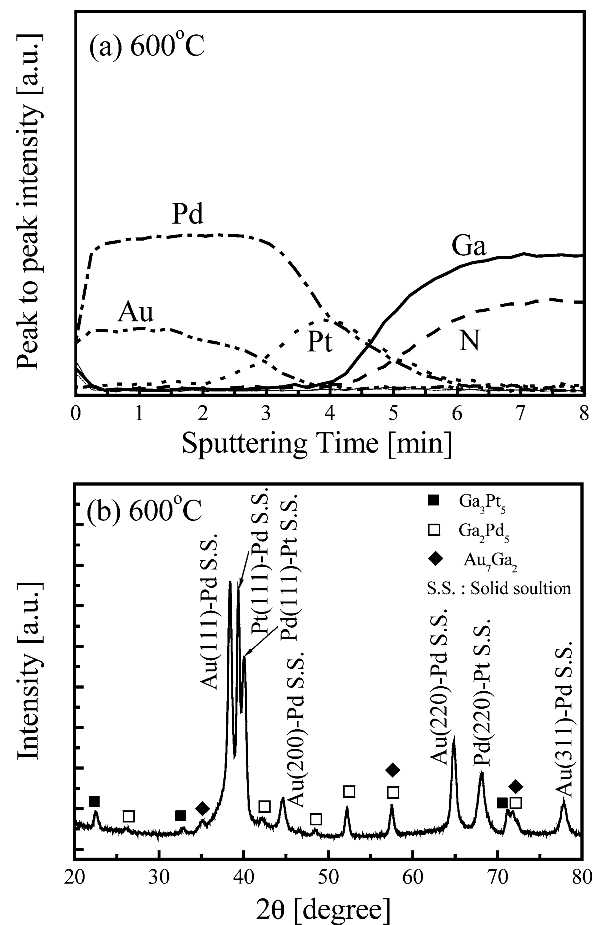

Fig. 5 (a) The AES depth profile of the sample annealed at 600°C. (b) The GXRD results of the sample annealed at 600°C, showing the formation of new phases such as Ga_3Pt_5, Ga_2Pd_5, and Au_7Ga_2

that Pt and Pd atoms easily react with Ga atoms and participated in the formation of Pt- and Pd-gallides, and/or Pt-Pd-gallides at the interface region. As for the Fig. 5(b), it is shown the GXRD plot of the sample annealed at 600°C. It is noteworthy that the intensity of the Au-based, Pd-based, and-Pt based solid solution peaks was dramatically increased, compared to that of the 500°C-annealed sample. In addition, there were new gallide phases, which were identified to be Ga_3Pt_5 (220)(22.5°), Ga_2Pd_5 (031)(26.25°), Ga_3Pt_5 (220)(32.90°), Ga_3Pt_5 (221)(40.06°), Ga_2Pd_5 (231)(42.17°), Ga_2Pd_5 (181)(48.42°), Ga_2Pd_5 (330)(52.22°), Ga_2Pd_5 (220)(57.51°), Au_7Ga_2 (210)(57.51°), Ga_3Pt_5 (422)(71.22°), Ga_2Pd_5 (123)(71.84°), and Au_7Ga_2 (413)(71.84°).

Based on the I-V characteristics, AES and GXRD results, correlation between interfacial reaction and electrical properties of the Pt/Pd/Au contacts on *p*-GaN could be explained as follows. The AES and GXRD results showed that the increase in the annealing temperature above 600°C leads to indiffusion of Pt, Pd, and Au atoms and formation of the Ga_3Pt_5, Ga_2Pd_5, and Au_7Ga_2 phases at the metal/GaN interface. This is in good agreement with those previously reported by other groups [19–29]. It is well known that for the Pt- and Pd-based contacts for p-GaN, Pt and Pd readily react with GaN and form Pd-Ga and Pt-Ga related phases upon annealing [19–29]. Mohney and Lin. also showed that the Pt- and Pd-gallides are particularly stable among the group VIII metal gallides, and so these metals are thermodynamically favored to react with Ga in GaN [31]. The outdiffusion of Ga atom and formation of Ga_3Pt_5, Ga_2Pd_5, and Au_7Ga_2 phases are indicative of the accumulation of Ga vacancies at the region near the surface of the p-GaN layer. This could lead to the formation of heavily p-doped region (p^+-GaN region) near the *p*-GaN surface, since Ga vacancies serve as deep-acceptors [32]. Thus, the increase in the carrier concentration at the surface region of the p-GaN by interface reactions could be responsible for the improved electrical properties of the 600°C annealed Pt/Pd/Au contact. Another possibility is related to the increase in the contact area due to the interfacial reactions between the metal layers and *p*-GaN [7, 8, 33]. Therefore, the improved specific contact resistivity

for 600°C contact can be related to the combined effects of the increases in the carrier concentration by Ga outdiffusion and the contact area.

4 Summary and conclusion

Electrical and structural properties of a Pt (5 nm)/Pd (5 nm)/Au (10 nm) contact on the p-GaN:Mg (2×10^{17} cm^{-3}) were investigated by using I-V measurement, AES depth profiles, and GXRD examination as a function of annealing temperature. The specific contact resistivity as low as $3.1 \times 10^{-5}\ \Omega\,\text{cm}^2$ was obtained from the samples when annealed at 600°C for 2 min in a N_2 ambient. Based on the AES and GXRD results, the ohmic behavior of the samples annealed at 600°C was explained in terms of the combined effects of the formation of Ga_3Pt_5, Ga_2Pd_5, and Au_7Ga_2 phases at the interface region, and the increase in the contact areas.

Acknowledgments This work is supported in part by US Air Force Office of Scientific Research (AFOSR)/Asian Office of Aerospace Research and Development (AOARD, monitor; Joanne Maurice).

References

1. S. Nakamura, M. Senoh, and T. Mukai, *Jpn. J. Appl. Phys.*, **32**, L8 (1993).
2. H. Amano, N. Sawaki, A. Akasaki, and Y. Toyoda, *Appl. Phys. Lett.*, **48**, 353 (1986).
3. K. Itoh, T. Kawamoto, H. Amano, K. Hiramatsu, and I. Akasaki, *Jpn. J. Appl. Phys.*, **30**, 1924 (1991).
4. S. Nakamura, T. Mukai, M. Senoh, S. Nagahama, and N. Iwasa, *J. Appl. Phys.*, **74**, 3911 (1993).
5. J.K. Ho, C.S. Jong, C.C. Chiu, C.N. Huang, C.Y. Chen, and K.K. Shih, *Appl. Phys. Lett.*, **74**, 1275 (1999).
6. J.K. Sheu, Y.K. Su, G.C. Chi, P.L. Koh, M.J. Jou, C.M. Chang, C.C. Liu, and W.C. Hung, *Appl. Phys. Lett.*, **74**, 2340 (1999).
7. J.-S. Jang, I.-S. Jang, H.-K. Kim, S. Lee, T.-Y. Seong, and S.-J. Park, *Appl. Phys. Lett.*, **74**, 70 (1999).
8. H.-K. Kim, T.-Y. Seong, and C.-R. Lee, *J. Electron. Mat.*, **148** (3), 266 (2001).
9. Y. Koide, H. Ishikawa, S. Kobayashi, S. Yamasaki, S. Nagai, J. Umezaki, M. Koike, and M. Murakami, *Appl. Surf. Sci.*, **117/118**, 373 (1997).
10. J.K. Sheu, Y.K. Su, G.C. Chi, W.C. Chen, C.Y. Chen, C.N. Huang, J.M. Hong, Y.C. Yu, C.W. Wang, and E.K. Lin, *J. Appl. Phys.*, **83**, 3172 (1998).
11. J.S. Kwak, K.Y. Lee, J.Y. Han, J. Cho, C. Chae, O.H. Nam, and Y. Park, *Appl. Phys. Lett.*, **79**, 3254 (2001).
12. J.K. Kim, J.-L. Lee, J.W. Lee, H.E. Shin, Y.J. Park, and T. Kim, *Appl. Phys. Lett.*, **73**, 2953 (1998).
13. J.-S. Jang, S.-J. Park, and T.-Y. Seong, *Appl. Phys. Lett.*, **76**, 2898 (2000).
14. J. Sun, K.A. Rickert, J.M. Redwing, A.B. Ellis, F.J. Himpsel, and T. F. Kuech, *Appl. Phys. Lett.*, **76**, 415 (2000).
15. J.-O. Song, D.-S. Leem,. J.S. Kwak, S.N. Lee, O.H. Nam, Y. Park, and T.-Y. Seong, *Appl. Phys. Lett.*, **84**, 1504 (2004).
16. J.-O. Song, D.-S. Leem, and T.-Y. Seong, *Appl. Phys. Lett.*, **83**, 3513 (2003).
17. J.-O. Song, D.-S. Leem, and T.-Y. Seong, *Appl. Phys. Lett.*, **84**, 4663 (2004).
18. D.-S. Leem, J.-O. Song, J.S. Kwak, Y. Park, and T.-Y. Seong, *Electrochem. Solid-State Lett.*, **7**, G210 (2004).
19. J.K. Kim, H.W. Jang, C.C. Kim. J.H. Je, K.A. Rickert, T.F. Kuech, J.-L. Lee, J. Vac. *Sci. Technol. B*, **21**, 87 (2003).
20. T. Arai, H. Sueyoshi, Y. Koide, M. Moriyama, and M. Murakami, *J. Appl. Phys.*, **89**, 2826 (2001).
21. J.K. Kim and J.-L. Lee, J. *Electrochem. Soc.*, **149**, G266 (2002).
22. L. Zhou, W. Lanford, A.T. Ping, I. Adesida, J.W. Yang, and A. Khan, *Appl. Phys. Lett*. **76**, 3451 (2000).
23. H.W. Jang, H.K. Cho, J.Y. Lee, and J.-L. Lee, *J. Electrochem. Soc.*, **150**, G212 (2003).
24. J.K. Kim, J.-L.Lee, J.W. Lee, H.E. Shin, Y.J. Park, and T. Kim, *Appl. Phys. Lett.*, **73**, 2953 (1998).
25. J.S. Kwak, O.-H. Nam, and Y. Park, *Appl. Phys. Lett.*, **80**, 3554 (2002).
26. H.-K. Kim, I. Adesida, and T.-Y. Seong, *J. Vac. Sci. Technol.*, **A22**, 1101 (2004).
27. H.-K. Kim., T.-Y. Seong, I. Adesida, C.W. Tang, and K.M. Lau, *Appl. Phys. Lett.*, **84**, 1710 (2004).
28. S. Murai, H. Masuda, Y. Koide, and M. Murakami, *Appl. Phys. Lett.*, **80**, 2934 (2002).
29. V. Adivarahan, A. Lunev, M.A. Khan, J. Yang, G. Simin, M.S. Shur, and R. Gaska, *Appl. Phys. Lett*. **78**, 2781 (2001).
30. J.-S. Jang, S.-J. Park, and T.-Y. Seong, *J. Vac. Sci. & Technol.*, **A 17**, 1668 (1999).
31. S.E. Mohney and X. Lin, *J. Electron. Mater.*, **25**, 811 (1996).
32. J. Sun, K.A. Rickert, J.M. Redwing, A.B. Ellis, F.J. Himpsel, T.F. Kuech, *Appl. Phys. Lett.*, **76**, 415 (2000).
33. H.-K. Kim, S.-H. Han, T.-Y. Seong, and W.-K. Choi, *Appl. Phys. Lett.*, **77**, 1647 (2000).